06

Features of photoelectric characteristics of CdS:Fe samples obtained using various techniques

© P.G. Kharitonova, S.V. Stetsyura

Saratov National Research State University,
410012 Saratov, Russia
e-mail: haritonovapg@gmail.com

Received December 22, 2025
Revised December 22, 2025
Accepted December 22, 2025

In this paper, we investigate heterophase CdS:Fe film samples obtained by thermal evaporation in vacuum and by a hybrid technique using the Langmuir–Blodgett technology. We conducted a comparative analysis of the photoelectric characteristics of the obtained samples, which showed significant differences in the nature of the change in dark currents and photocurrents when using the specified methods for obtaining samples. The observed differences in the values of the dark current and photocurrent, photosensitivity and photocurrent changes over time are explained by the different arrangement of the layers that are the source of Fe during diffusion, and, as a result, the different arrangement of the heterophase region with nanoscale FeS inclusions relative to the illuminated surface of the sample. As a result of diffusion and precipitation processes in the first case (Langmuir–Blodgett technology), the largest nanoscale FeS precipitates are formed near the illuminated surface, and in the second case (thermal evaporation in vacuum), they are formed near the substrate. The advantages of a hybrid method of obtained CdS:Fe for synthesis a material with an extended range of properties and high photosensitivity have been revealed.

Keywords: iron-doped cadmium sulfide, photoelectric characteristics, thermal evaporation in vacuum, Langmuir–Blodgett layers.

DOI: 10.61011/TP.2026.05.63520.341-25

Introduction

Due to their specific chemical, electronic, optical and magnetic properties, nanocrystalline semiconductive thin films are studied today in many fundamental and applied research [1–3]. One of the most talked about and used nanocrystalline semiconductor films are the films based on cadmium sulfide (CdS) — a wideband semiconductor of group II−VI with a band gap of 2.42 eV at room temperature. CdS is in demand in a wide range of applications, including optical detectors, photovoltaic cells, sensors with extended functional capabilities [4–6].

For the fabrication of CdS thin films, both physical and chemical methods are used [7,8]. Among the chemical methods, chemical bath deposition method stands out, which can be provided over large areas and at low temperatures. By selecting the appropriate deposition parameters such as pH, bath temperature, reaction time, mixing duration, and the amount of doping impurities and complexing agents introduced in a special way: This method can be used to fabricate high-performance nanocrystalline semiconductor films with controlled surface density and required nanoparticle sizes [9–11]. Arrangment of the substrate inside the reactor also plays an important role in the formation of CdS films. In the study [12], it was shown that selecting the substrate position allowed to lower the number of precursor solutions and, thus, reduce the amount of toxic waste generated. Another promising method to obtain CdS films is the method of radio frequency magnetron sputtering.

In [13] it was demonstrated that CdS films grown on ultrathin glass substrates using radio frequency magnetron sputtering were characterized by high crystallinity, large optical band gap (2.40 eV), symmetrical surface, uniform grain growth, low resistivity ($3.16 \cdot 10^4\,\Omega \cdot \mathrm{cm}$) and high concentration of charge carriers ($5.56 \cdot 10^{13}\,\mathrm{cm}^{-3}$).

Alloying with metal atoms, including transition metals such as Mn, Ni, and Fe, is successfully used to control the chemical and physical characteristics of CdS thin films, which create intermediate energy states in the band structures of semiconductor films, thereby affecting their magnetic, electrical, and optical characteristics [14–16]. Currently, CdS films doped with iron (CdS:Fe) are of the greatest interest for research. In particular, in [17] CdS:Fe films were obtained by aerosol pyrolysis using iron nitrate, chloride, and sulfate as iron precursors. Based on experimental data and thermodynamic analysis, the authors of the article have established that the composition, uniformity and morphology of the surface of CdS:Fe films significantly depends on the nature of the iron precursor. The presence of Fe dopants led to an increase in the optical band gap of CdS:Fe to 2.44−2.49 eV. The obtained films, according to the authors, are well suited as ligatures for the manufacture of Fe:ZnSe laser elements. In [18], the effect of gamma irradiation on the optical, morphological, and structural characteristics of thin nanostructured CdS films and CdS films doped with Fe was studied. For

the obtained samples, a decrease in the grain size of the films was observed with an increase in Fe concentration and their increase with higher radiation dose. It was found that the broadband radiation peak for the thin films of „pure“ CdS was located in 500−650 nm centered at a wavelength of 542 nm, and for CdS films doped with Fe, three different radiation bands were characteristic with centers at wavelengths of 400, 467 and 530−540 nm, which corresponded to the occurrence of permitted Fe levels in CdS band gap.

By doping CdS with iron it is possible to obtain the so called diluted magnetic semiconductors (DMS) both, as solid solutions and as heterophase structures on its basis. Depending on the technologies used, the researchers were able to obtain both, solid solutions $Cd_xFe_{1-x}S$ and CdS-FeS [19] nanocomposites with various ferromagnetic, optical, and photoelectric properties. Since Fe doping should lead to the occurrence of magnetic properties, these properties, as a rule, were studied primarily in [20]. The magnetic properties of fabricated CdS:Fe are outlined in [21,22]. Such DMS are promising candidates for creating magneto-optical devices, non-volatile storage devices, biosensors, and spintronic devices on their basis [23,24].

Photovoltaic characteristics of CdS:Fe has been given attention in a number of papers [25–27], and the results obtained indicate the prospects for their study. The analysis of these papers indicates a significant influence of the fabrication method on the photovoltaic characteristics of CDs:Fe material. For example, [25] describes the suppression of photoconductivity in CdS thin films doped with iron obtained by spray pyrolysis. The authors showed that Fe dopants in a certain concentration act as centers of quenching of CdS photoconductivity, and with a large fraction of FeS phase, the photosensitivity of material in the visible wavelength range almost disappears. Since photosensitivity was maintained and performance increased at low concentrations of Fe as a dopant, the authors of [25] suggested that CdS:Fe film structures may be used in optical sensors that require a fast response and return to normal when illumination was switched off. It should be emphasized that the authors did not pay attention to possible heterogeneity of the chemical and phase compositions of the structures when analyzing the photovoltaic characteristics.

Thus, it was demonstrated earlier that it was possible to obtain new functionality or significantly improve the characteristics of CdS-based materials by using iron as a doping agent. In particular, we obtained CdS:Fe materials using both, thermal vacuum evaporation (TVE) [21], and Langmuir-Blodgett (LB) methods [28]. The prospects of both methods for creating magneto and photosensitive samples were shown, but no comparison and analysis of the photovoltaic characteristics was made for CdS:Fe samples fabricated using various techniques, which was the purpose of this article.

1. Materials and technologies

In this study, modified and unmodified polycrystalline film structures based on CdS films fabricated by TVE method on a mica substrate were obtained and studied. The CdS film was modified by creating a nanometer-thick iron-containing layer adjacent to the CdS film and subsequent annealing of the structure. Moreover, the iron-containing layer was created either in the same way as the CdS layer using TVE method or using LB method.

Let's consider each method in detail.

The basis of each studied structure was a polycrystalline CdS film with a thickness of about $2\,\mu$m, deposited on a mica substrate using TVE method. Thermal spraying of the films took place in „open volume“ on a multipurpose setup VUP-5. Powdered CdS of semiconductor purity class was used to prepare the blend. $CuCl_2$ in the amount of 0.1 wt.% was added to the blend as an activator. Next, the blend was placed in a crucible and thoroughly mixed. The mentioned films were fabricated at a substrate temperature of 80 °C−100 °C and evaporator temperature of 780 °C. The evaporator coil was heated by a gradual increase in voltage across it from 0 to 200 V. The sputtering was made in the chamber at a pressure of $6.5 \cdot 10^{-4}$ Torr. As a result, films with a nanocrystalline structure of cubic modification, insensitive to illumination, were obtained. The sensing was carried out by annealing in air at a temperature of (540 ± 5) °C for 15 min. During thermal annealing in air, a phase transition from cubic modification (sphalerite) to hexagonal (wurtzite) was observed for CdS, which occurred gradually in the temperature range from 250 °C to 700 °C [29,30].

Thus, the first batch of „pure“ CdS film samples was obtained, with the photoelectric characteristics and light stability of which the corresponding characteristics of heterophase CdS:Fe samples were compared, with their fabrication and research described in this paper.

The second batch of samples was obtained using only TVE technology alone when applying the film structure layer by layer. Compared to fabrication of „pure“ CdS described above, first, a layer of chemically pure Fe 30−50 nm thick was applied onto the mica substrate and only after that — CdS layer. Thus, the film, which was the source of iron during diffusion, was located between the mica substrate and the CdS film. After that, the multi-layer film structures were also subjected to a high-temperature annealing in the air at a temperature of (450 ± 5) °C during 15 min. During the process of annealing, photosensitive crystallites CdS [29,30] grew and recrystallized, Fe atoms diffused deep into CdS, the solid solution of $Cd_xFe_{1-x}S$ was formed, and Fe and Cd were oxidized in open surface, which was confirmed by our research using electron and atomic force microscopy, secondary ion mass spectrometry, and Auger spectroscopy, energy dispersion analysis, and outlined in [21]. These structures are schematically shown in Fig. 1, *a*.

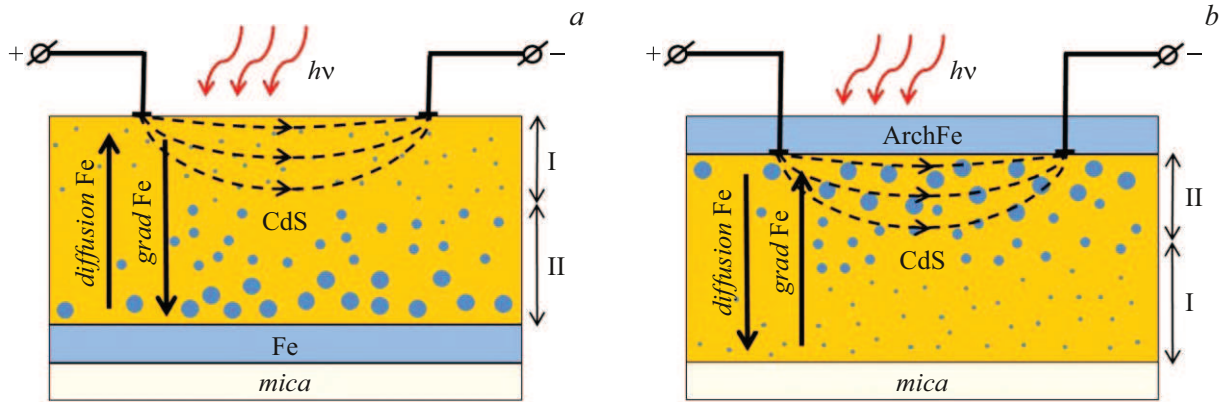

Figure 1. Schematic representation of samples obtained using: *a* — TVE method; *b* — hybrid method of TVE/LB. The vertical arrows show the direction of diffusion and the gradient of Fe concentrations that occur during annealing. Region I — region of CdS:Fe solid solution, region II — region of FeS nanoparticles precipitation.

The third batch of samples was fabricated using TVE/LB hybrid method, when the CdS layer was obtained by TVE on a mica substrate using the above-described mode, and then an iron-containing coating was applied to the surface of the CdS layer by LB method. These structures are schematically shown in Fig. 1, *b*.

LB technology and its capabilities are described in [31]. The studied samples were obtained as follows. To obtain organic coatings structured with iron, a film of monolayers of iron arachinate (ArchFe), obtained by LB method, was deposited on CdS. To form the monolayers, arachic acid (produced by Sigma Aldrich) was used, which was diluted in chloroform to a concentration of 10^{-3} mol/l. Deionized water and salt $FeCl_3$ (Sigma Aldrich, chemically pure class) were used in fabrication of the sub-phase. The concentration and pH $FeCl_3$ in water solution was 10^{-3} mol/l and (4.2 ± 0.05) respectively. The indicated concentrations, amounts, and pH of $FeCl_3$ aqueous solution were selected based on previous experiments and literature data [28], which ensured the formation of a tightly packed monolayer of ArchFe on the surface of the aqueous subphase. The arachic acid in chloroform was introduced on the surface of water subphase $FeCl_3$ in the amount of 50 μl.

To fabricate, control the quality and transfer the monolayers they used KSV-Nima LB Through Medium KN 2002 (KSV-Nima, Finland) setup fitted with two movable barriers. The monolayer on the surface of the aqueous subphase was compressed at a rate of 25 mm/min until a tightly packed monolayer was formed. The quality of obtained monolayers was checked using π-A-isotherms. The transfer of iron-containing monolayers to a solid substrate was carried out while maintaining the given surface pressure of 17 mN/m, which was determined by weighing the Wilhelmi plate with an accuracy of 0.01 mN/m. The air and subphase temperature $(23 \pm 1)\,^{\circ}$C was kept constant. ArchFe monolayers were transferred to a polycrystalline CdS film by the Langmuir-Schaeffer method, in which the substrate is oriented almost horizontally and is brought into easy contact with the monolayer. A multilayer of *X*-type could be obtained by repeating this operation. To increase the surface density of Fe, 30 monolayers of ArchFe were deposited on CdS surface. The presence of Fe and its surface density were controlled by energy dispersion analysis methods at all stages of [27]. After that CdS films with ArchFe coating were annealed at a temperature of $(545 \pm 5)\,^{\circ}$C during 15 min. During annealing, organic matter was oxidized and decomposed to form volatile compounds, and Fe atoms were diffused deep into CdS. The presence of Fe and its surface density were also controlled by energy dispersion analysis methods. At the end of annealing, ArchFe layer shown in Fig. 1, *b* practically disappeared and lost its continuity — the organic component sublimated, the density of Fe atoms registered on the surface decreased by more than an order of magnitude, while the distribution of Fe atoms over the sample depth was registered by the secondary ion mass method-spectrometry [27].

Figure 1 shows the differences in the structures of the obtained samples and their phase heterogeneity in depth, depending on the fabrication method. In the first case, when using only TVE method to create the studied structures (Fig. 1, *a*), the diffusion of iron atoms took place from a limited source located between the mica substrate and CdS film, deep into CdS and was directed to the surface of the film. The gradient of Fe concentration in the final (annealed) structure is oriented in the opposite direction — from the illuminated (working) surface of CdS to the substrate. In this case, the precipitation of Fe atoms and the formation of FeS nanoclusions occur at the substrate (i.e., in the depth of CdS), and the formation of a solid solution of substitution $Cd_xFe_{1-x}S$ — at the surface due to the low concentration of Fe, which does not exceed its limiting solubility in CdS.

In the second case, when using TVE/LB hybrid technique to create the studied structures (Fig. 1, *b*), an iron-containing film being a source for diffusion, was applied over a polycrystalline CdS film. In this case, the diffusion of iron atoms was directed deep into CdS towards the substrate.

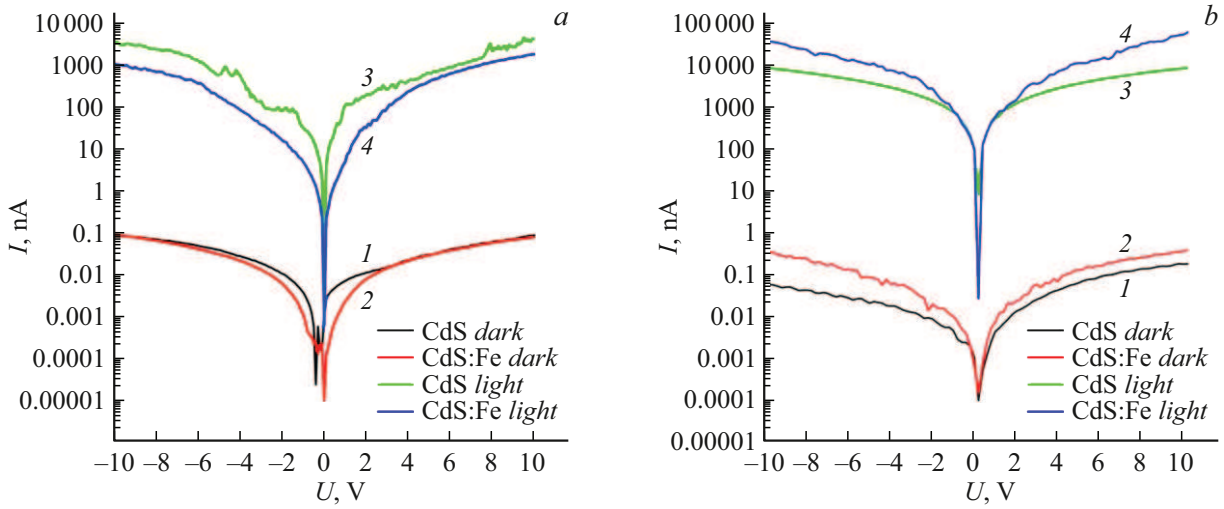

Figure 2. . VAC curves measured in darkness (curves *1*, *2*) and under illumination (curves *3*, *4*) plotted in a semilogarithmic scale, for samples of „pure“ CdS (curves 1,3) and heterophase film samples of CdS:Fe (curves *2*, *4*) obtained using: *a* — TVE technology; *b* — TVE/LB hybrid method..

Larger iron-containing inclusions were formed near the surface; their sizes diminished with depth, and a region of solid solution $Cd_xFe_{1-x}S$ was located closer to the substrate.

All the described processes of Fe diffusion in CdS and the precipitation of FeS nanoinclusions with an estimate of the precipitates' geometry depending on their occurrence depth were modeled and experimentally proved in [27].

It is expected that the location of the heterophase region closer to the surface or substrate of the sample should have a different effect on the photovoltaic characteristics and their light stability. At the same time, the expected change is not trivial and is completely predictable, since the result is jointly affected by several processes that depend on the chemical and phase compositions of the CdS:Fe film material that are heterogeneous in depth, as well as the level of its exposure.

2. Study of photoelectric dependencies

The photovoltaic characteristics were measured using a probe station Cascade Microtech RM-5 probe and Agilent B1500A analyzer. The probe station made it possible to measure the volt-ampere characteristics (VAC) with a required precision without applying metal contact pads to the surface of hybrid structures: the distance on the studied samples surface between the probe contacts was maintained constant and equal to 0.8mm. Motic MLK-150C halogen lamp was used to illuminate the samples during measurements, providing an illumination intensity in the plane of the sample surface of 20,000 lx. The directions of the luminous flux and the lines of electric field strength shown as dotted lines in Fig. 1 in the corresponding samples were mutually perpendicular, which corresponded to the transverse mode of photoconductivity. The transverse mode of photoconductivity is outlined in more detail in [29]. The electric field strength lines shown in Fig. 1, together with the directions of illumination, shed light not only on the transverse mode of photoconductivity, but also on the sample areas through which current flows predominantly in this mode.

It should be stressed that in case of transverse photoconductivity, current flows through the near-surface layers of the semiconductor (up to $1\,\mu$m thick), in which the resistance changes most effectively when illuminated (the light absorption coefficient for CdS in visible range is $(5.5-7.0)\cdot 10^4\,\mathrm{cm}^{-1}$) [29]. The voltage between the contacts varied from -10 to $+10$ V with a step of 0.1 V.

Figure 2 shows typical VAC measured under illumination and in the dark for „pure“ CdS samples and heterophase CdS:Fe film samples obtained using TVE technology and TVE/LB hybrid method. Due to significant photosensitivity of the samples and the current values, which vary by orders of magnitude with modification of CdS composition and illumination, semilogarithmic scale of the graphs was used. From Fig. 2, *a* it can be seen that dark currents and currents under illumination in CdS:Fe samples were obtained using only TVE method and having an equivalent structure Fig. 1, *a*, are slightly less than for „pure“ CdS, especially at low voltages. For CdS:Fe samples fabricated by TVE/LB hybrid method (Fig. 2, *b*), dark and „light“ currents exceed the currents for „pure“ CdS over the entire voltage range, and more noticeably at high voltage values.

As seen from the Fig. 2 the dark currents passing through the samples of „pure“ CdS (I_{dark_0}) and modified samples of CdS:Fe (I_{dark},) obtained by various methods were compared. D, L, and k parameters have been introduced to help quantify changes in the photovoltaic characteristics of the studied samples. Parameter D, corresponding to the ratio I_{dark_0}/I_{dark}, illustrates how CdS modification

Parameters D, L, k for the samples of „pure“ CdS and heterophase film samples of CdS:Fe fabricated using TVE method (CdS:Fe (TVE)) and hybrid method of TVE/LB (CdS:Fe (TVE/LB))

Sample type	D	L	k
CdS	–	–	$2.4 \cdot 10^4 - 4.5 \cdot 10^4$
CdS:Fe (TVE)	1.1–1.4	3.0–6.0	$1.8 \cdot 10^4 - 3.2 \cdot 10^4$
CdS:Fe (TVE/LB)	0.49–0.55	0.09–0.14	$7.0 \cdot 10^4 - 14.6 \cdot 10^4$

method influences the dark currents and the dark resistances, accordingly. Also, the values of L were analyzed corresponding to the ratio I_{light_0}/I_{light}, where I_{light_0} — value of photocurrent under illumination of 20 000 lx, passing through „pure“ CdS, and I_{light} — photocurrent passing through the modified CdS:Fe sample at the same level of illumination. The values of these parameters are given in the Table below. Since the changes in dark currents and photocurrents vary depending on the voltages, the table shows the range of values obtained. Also, the table gives the values of parameter k — ratios of photocurrent I_{light} under illumination of 20 000 lx — to the value of dark current I_{dark} for each of the studied structures. The values of k parameter indicate the photosensitivity of the test sample, i.e. a change in the electrical conductivity of the test film when exposed to light.

Apparently, the values of D and L, which are less than one, evidence an increase in the corresponding currents in CdS:Fe samples compared to the initial unmodified CdS films.

It follows from the table that in CdS:Fe (TVE) samples the dark current decreased by 10 %–40 % compared to the initial CdS film, which may be associated with a higher resistance due to the formation of additional Fe recombination levels in CdS band gap during the formation of $Cd_xFe_{1-x}S$ substitution solid solution in the near-surface region of the sample (Fig. 1, *a*). Light current values also decreased due to the increased recombination rate, resulting in a diminished photosensitivity at 25 %–28 %. The formation of recombination levels during introduction of Fe into CdS and the formation of a solid solution is indirectly proved by publications [25,32,33], in which the authors studied the luminescence and absorption spectra of CdS and CdS:Fe. Thus, in the article [32] based on the change in the absorption and luminescence spectra, the authors concluded that energy levels of the dopant Fe appeared, corresponding to the red emission peak near 640 nm, and the number of induced sublevels increased with a growing concentration of Fe. The authors [25] found that doping of CdS with iron is an important parameter for the occurrence of new photoluminescence peaks and quenching of the main peak in CdS crystals with Fe. The authors associate this effect with positively charged excited centers of Fe. Following the authors [33], who observed a luminescence band caused by divalent iron ions with a maximum peak at 707.9 nm, the authors [25] concluded that Fe acts as a killer center (a recombination center, capturing electrons and holes) in CdS and quenches or significantly diminishes the luminescence phenomena.

For CdS:Fe (TVE/LB) samples, the dark current did not decrease compared to the initial unmodified CdS sample, but grew by approximately 1.8–2.0 times, which can be explained by a lower resistance in CdS:Fe (TVE/LB) film because of formation of more conductive, compared to CdS, iron-containing nanoclusters on its surface (Fig. 1, *b*), but, as follows from the table and Fig. 2, *b*, the photocurrents in the modified sample also increased significantly, and a way more significantly than the dark currents, which led to the growth of photosensitivity of CdS:Fe compared to the initial „pure“ CdS film by 7–14 times. The effect of increasing photosensitivity can be explained by the fact that light absorption occurs in the region of FeS precipitates formation (Fig. 1, *b*). The effect of current change in multiple times upon illumination in heterophase materials and structures can be caused by various mechanisms and was observed earlier for both organic [34] and inorganic [35] and hybrid materials. For example, a similar effect was previously observed in heterophase materials CdS–PbS [36] and was explained by a decline in the recombination rate of nonequilibrium charge carriers due to the outflow of radiation and technological defects into nanosized inclusions of PbS [37,38].

In addition to the analysis of the current-voltage characteristics (stationary approach), also, the kinetic characteristics of the current were studied to determine their light instability peculiar to many photosensitive materials. The measurements were carried out with the switched on illumination with intensity of 20 000 lx for 7.5 min with a periodic light switching off for 7.5 min under constant voltage −6 V. The total time of illumination was 30 min. The obtained current versus time curves are given in Fig. 3.

By light instability we mean the change in the photoelectric characteristics of a semiconductor sample over time at constant illumination, depending on the sample's illumination history or duration of illumination. One of the signs of light instability is photofatigue of a semiconductor material that was exposed to a light flux for a long time [38]. Photofatigue is understood as a decline in photocurrent through a sample during illumination with a constant intensity. Photofatigue is calculated as the ratio of photocurrents at a given voltage before and after

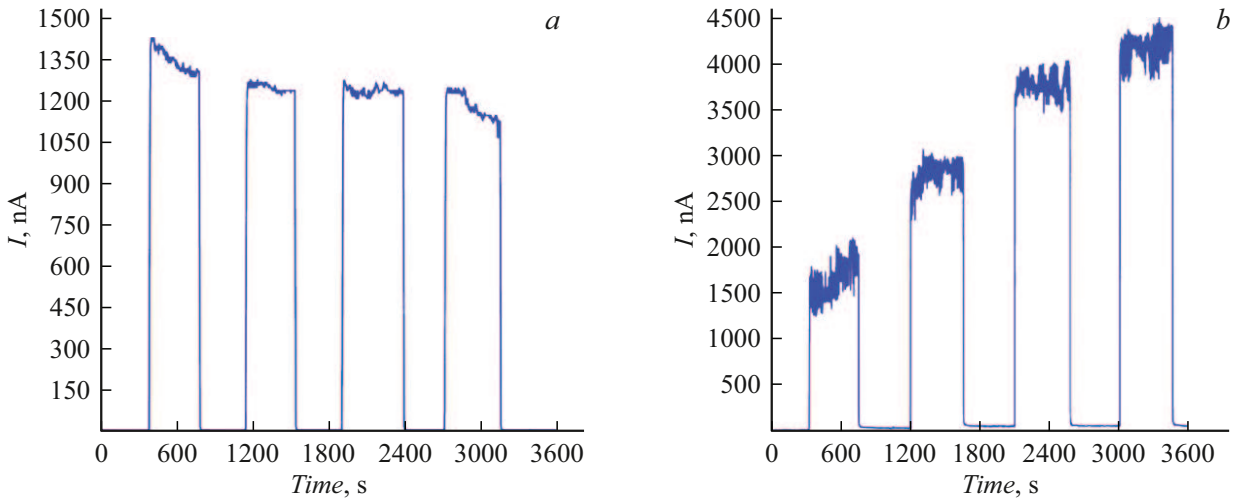

Figure 3. Dependences of current on time during periodic switching on of illumination with the same intensity for CdS:Fe obtained: *a* — by the TVE method; *b* — by method using LB technology (TVE/LB).

illumination of the sample. If the photofatigue coefficient is greater than one, this usually indicates degradation of photosensitivity (a decline in photocurrent and an increase in dark current). There are known cases of the so-called negative photofatigue [37,38], when after prolonged exposure the photocurrent rises, but the photosensitivity (the ratio of photocurrent to dark current at a given voltage) increases or remains constant.

For CdS:Fe obtained by TVE method, when the illumination is turned on, a small (up to 5%) photofatigue (a decrease in current over time at a fixed illumination) typical for CdS is observed, which is clearly visible in Fig. 3, *a*. This adversely affects the material photosensitivity. At the same time, the values of light and dark currents also decreased slightly from pulse to pulse.

For a heterophase CdS:Fe (TVE/LB) sample at the surface, obtained using a hybrid method, the type of current dependence on time with periodic switching on of illumination is noticeably different (Fig. 3, *b*). When the light was switched on, both during one pulse and from pulse to pulse, the photocurrent tended to increase rather than decrease — during the pulsed illumination (a total of 30 min), the photocurrent grew on average 60 % of the initial value every time the light was switched on, and over the entire illumination period this increase was 200 %. A similar effect, called „negative photofatigue“ [37], was previously observed by several groups of authors in heterophase materials based on CdS [37,38] and was explained by the presence of narrow-band nanoscale inclusions [37] and the occurrence of specific photochemical reactions [38]. Significant changes in photocurrents can be associated with such a photochemical reaction as the photostimulated release of donors from drains (FeS) into the main volume of CdS film. This reaction is characterized by a fairly long characteristic process time, but further research is required to confirm this assumption.

Conclusion

Thus, in this study, the photoelectric characteristics of CdS:Fe film samples obtained by TVE and using a technique including the LB method. A comparative analysis of dark currents and photocurrents in stationary and kinetic modes was carried out for the „pure“ polycrystalline CdS films and heterophase CdS:Fe samples. A comparison of the photoelectric characteristics and parameters of CdS:Fe samples obtained by different methods showed that both batches of samples have photosensitivity in the visible region of the spectrum, but the nature of the change in currents is diametrically opposed: the dark currents and photocurrents of heterophase CdS:Fe samples fabricated by TVE method decline, while for the films obtained by hybrid technology they increase. Over time, under constant illumination, the sensitivity of CdS:Fe samples obtained using TVE method decreases slightly. For CdS:Fe samples obtained using the hybrid TVE/LB method, the phenomenon of negative photofatigue is observed in the kinetic dependences. The observed differences are explained by different location of the precipitation region of FeS nanoinclusions relative to the illuminated surface of the sample. After diffusion in the first case (LB technology), the largest nanosized FeS precipitates are formed near the illuminated surface, and in the second case (thermal evaporation in a vacuum) they are formed closer to the substrate.

Thus, the prospects of a hybrid technique using LB method for the formation of CdS–FeS heterophase structure are highlighted, the use of which made it possible to create a material with an extended range of properties and not only preserve, but also increase the material photosensitivity by more than an order of magnitude. The algorithm for obtaining heterophase CdS–FeS films using only TVE method, considered herein, may turn out to be effective only for ultra-thin CdS films (thickness less than 1 μm),

since in this case it is possible to expand the precipitation region to the thickness of the entire film.

Funding

Some parts of this study were made supported financially by the Russian Science Foundation — grant № 22-22-00194, https://rscf.ru/project/22-22-00194/.

Conflict of interest

The authors declare that they have no conflict of interest.

References

[1] M. Sharma, J. Panigrahi, V.K. Komarala. Nanoscale Adv., **3** (12), 3373 (2021). DOI: 10.1039/d0na00791a
[2] C. Cao, Q. An. Cryst. Eng. Comm., **27** (21), 3404 (2025). DOI: 10.1039/D5CE00244C
[3] M. Hou, Z. Zhou, A. Xu, K. Xiao, J. Li, D. Qin, W. Xu, L. Hou. Nanomaterials, **11** (8), 2071 (2021). DOI: 10.3390/nano11082071
[4] A. Bosio, G. Rosa, N. Romeo. Solar Energy, **175**, 31 (2018). DOI: 10.1016/j.solener.2018.01.018
[5] F. Gode, S. Unlu. Mater. Sci. Semicond. Process., **90**, 92 (2019). DOI: 10.1016/j.mssp.2018.10.011
[6] A. Ashok, G. Regmi, A. Romero-Núnez, M. Solis-Lopez, S. Velumani, H. Castaneda. J. Mater. Sci.: Mater. Electron., **31** (10), 7499 (2020). DOI: 10.1007/s10854-020-03024-3
[7] F.M. Ahmed, A.M. Muhammed Ali, R.A. Ismail, M.A. Fakhri, E.T. Salim. J. Mater. Sci.: Mater. Electron., **34**, 1906 (2023). DOI: 10.1007/s10854-023-11380-z
[8] M.A.K.L. Dissanayake, K. Paramanathan, G.K.R. Senadeera, C.A. Thotawattage, K. Balashangar, P. Ravirajan, B.S. Dassanayake. Thin Solid Films, **791**, 140225 (2024). DOI: 10.1016/j.tsf.2024.140225
[9] K.A. Aloueedat, N.M. Ahmed, M.R.B. Omer, K. Daoudi, M.A. Almessiere. Optik, **300**, 171657 (2024). DOI: 10.1016/j.ijleo.2024.171657
[10] S.M. Pawar, B.S. Pawar, J.H. Kim, Oh-Shim Joo, C.D. Lokhande. Current Appl. Phys., **11** (2), 117 (2011). DOI: 10.1016/j.cap.2010.07.007
[11] M. Shabana, M. Mustafaa, A.M. El Sayed. Mater. Sci. Semicond. Process., **56**, 329 (2016). DOI: 10.1016/j.mssp.2016.09.006
[12] R.C. Ruiz-Ortega, L.A. Esquivel-Mendez, M.A. Gonzalez-Trujillo, C. Hernandez-Vasquez, Y. Matsumoto, M.D.L. Albor Aguilera. ACS Omega, **8** (35), 31725 (2023). DOI: 10.1021/acsomega.3c02158
[13] C. Doroody, K.S. Rahman, H.N. Rosly, M.N. Harif, M. Isah, Y.B. Kar, S.K. Tiong, N. Amin. Mater. Sci. Semicond. Process., **133**, 105935 (2021). DOI: 10.1016/j.mssp.2021.105935
[14] Z. Pan, S. Wang, R. Yan, C. Song, Y. Jin, G. Huang, J. Huang. Opt. Mater., **109**, 110324 (2020). DOI: 10.1016/j.optmat.2020.110324
[15] S. Yılmaz, M. Tomakin, A. Ünverdi, A. Aydın, I. Polat, E. Bacaksız. J. Mater. Sci.: Mater. Electron., **31** (15), 12932 (2020). DOI: 10.1007/s10854-020-03846-1
[16] S. Chandramohan, A. Kanjilal, S.N. Sarangi, S. Majumder, R. Sathyamoorthy, T. Som. Appl. Phys. A, **99**, 837 (2010). DOI: 10.1007/s00339-010-5598-z
[17] T.S. Volkov, E.M. Gavrishchyk, A.M. Kut'in, D.V. Savin, A.V. Nezhdanov, A.S. Markelov, A.I. Mashin, S.V. Kurashkin. Phys. B: Condensed Matter, **688**, 416140 (2024). DOI: 10.1016/j.physb.2024.416140
[18] T. Tohidi, N. Yousefpour Novini, K. Jamshidi-Ghaleh. Opt. Mater., **151**, 115394 (2024). DOI: 10.1016/j.optmat.2024.115394
[19] Y. Li, S. Chen, K. Zhang, S. Gu, J. Cao, Y. Xia, C. Yang, W. Sun, Z. Zhou. New J. Chem., **44** (34), 1144 (2020). DOI: 10.1039/D0NJ01424A
[20] K. Kaur, G.S. Lotey, N.K. Verma. J. Mater. Sci.: Mater. Electron., **25** (6), 2605 (2014). DOI: 10.1007/s10854-014-1918-y
[21] S.V. Stetsyura, P.G. Kharitonova, I.V. Malyar. Appl. Phys., **5**, 66 (2020).
[22] S.V. Stetsyura, P.G. Kharitonova. St. Petersburg State Polytechnical Univer. J. Phys. Mathem., **16** (1.2), 236 (2023). DOI: 10.18721/JPM.161.236
[23] A. Bukhtiar, B. Zou. Mater. Adv., **5** (17), 6739 (2024). DOI: 10.1039/D4MA00523F
[24] R. Khan, I. Shigidi, S. Al Otaibi, K. Althubeiti, S.S. Abdullaev, N. Rahman, Mohammad sohail, A. Khan, S. Iqbal, T. Del Rosso, Q. Zaman A. Khan. RSC Adv., **12** (55), 36126 (2022). DOI: 10.1039/D2RA06637H
[25] N. Badera, B. Godbole, S.B. Srivastava, P.N. Vishwakarma, L.S. Sharath Chandra, D. Jain, M. Gangrade, T. Shripathi, V.G. Sathe, V. Ganesan. Appl. Surf. Sci., **254** (21), 7042 (2008). DOI: 10.1016/j.apsusc.2008.05.218
[26] P.G. Kharitonova, E.G. Glukhovskoy, A.V. Kozlowski, S.V. Stetsyura, Semiconductors, **57** (7), 510 (2023). DOI: 10.61011/SC.2023.07.57411.4912C
[27] S.V. Stetsyura, P.G. Kharitonova, A.M. Zakharevich. Tech. Phys., **70** (5), 881 (2025). DOI: 10.61011/TP.2025.05.61125.471-24
[28] S.V. Stetsyura, P.G. Kharitonova, E.G. Glukhovskoy. St. Petersburg State Polytechnical Univer. J. Phys. Mathem., **15** (3.3), 250 (2022). DOI: 10.18721/JPM.153.349
[29] Z.I. Kiryashkina, A.G. Rokah, N.B. Katz, V.P. Malkov, E.A. Novikova, N.M. Tsukerman. *Fotoprovodyaschiye plenki (tipa CdS)* (Saratov University, Saratov, 1979) (in Russian)
[30] G. Hass, R.E. Tun. *Fizika tonkykh plenok* (Mir, M., 1968), v. 3, p. 332 (in Russian).
[31] A.I. Yanklovich. V sbor. *Uspekhi colloidnoy chemii*, ed. by A.I. Rusanova (Khimiya, L., 1991) (in Russian).
[32] M. Shkir, T. Alshahrani. J. Phys. Chem. Solids, **177**, 111282 (2023). DOI: 10.1016/j.jpcs.2023.111282
[33] B. Tripathi, F. Singh, D.K. Avasthi, A.K. Bhati, D. Das, Y.K. Vijay. J. Alloys Compounds, **454** (1−2), 97 (2008). DOI: 10.1016/j.jallcom.2007.01.016
[34] S.G. Yudin, V.V. Bodnarchuk, V.V. Lazarev, A.I. Smirnova, S.V. Yablonskii. Liquid Crystals and their Application, **19** (4), 50 (2019). DOI: 10.18083/LCAppl.2019.4.50
[35] A.G. Rokakh, S.V. Stetsyura. Inorganic Mater., **33** (2), 153 (1997).
[36] A.G. Rokakh. Pis'ma v ZhTF, **10** (13), 820 (1984) (in Russian).
[37] A.G. Rokakh, S.V. Stetsyura, A.A. Serdobintsev. Izvestiya of Saratov University. Physics, **5** (1), 92 (2005) (in Russian). DOI: 10.18500/1817-3020-2005-5-1-92-102
[38] M.K. Sheinkman, N.E. Korsunskaya. *Fotokhimicheskiye reaktsii v poluprovodnikakh tipa A2B6*. In book Fyzika soyedineniy A2B6, edited by A.N. Georgobiani, M.K. Sheinkman (Nauka, M., 1986) (in Russian).

Translated by T.Zorina